

# CROSS SECTION OF THE $^{144}\text{Sm}(n,\alpha)^{141}\text{Nd}$ REACTION AT 4.0, 5.0, AND 6.0 MeV

Yu.M. Gledenov, M.V. Sedysheva

*Frank Laboratory of Neutron Physics, Joint Institute for Nuclear Research, Dubna 141980, Russia*

Guohui Zhang, Zhimin Wang, Xiao Fan, Luyu Zhang, Huaiyong Bai, Jinxiang Chen  
*State Key Laboratory of Nuclear Physics and Technology, Institute of Heavy Ion Physics,  
Peking University, Beijing 100871, China*

L. Krupa<sup>a,b</sup>

<sup>a)</sup>*Flerov Laboratory of Nuclear Reactions, Joint Institute for Nuclear Research, Dubna 141980*

<sup>b)</sup>*Institute of Experimental and Applied Physics, Czech Technical University in Prague,  
Horska 3a/22, Prague 2, 12800 Czech Republic*

G. Khuukhenkhoo

*Nuclear Research Centre, National University of Mongolia, Ulaanbaatar, Mongolia*

## ABSTRACT

Cross sections of the  $^{144}\text{Sm}(n,\alpha)^{141}\text{Nd}$  reaction were measured at  $E_n = 4.0, 5.0$  and  $6.0$  MeV performed at the 4.5-MV Van de Graaff Accelerator of Peking University, China. A double-section gridded ionization chamber was used to detect the alpha particles. The samples of  $^{144}\text{Sm}_2\text{O}_3$  were placed at the common cathode plate of the chamber. Monoenergetic neutrons were produced by a deuterium gas target through the  $^2\text{H}(d,n)^3\text{He}$  reaction. The neutron flux was monitored by a  $\text{BF}_3$  long counter. Cross sections of the  $^{238}\text{U}(n,f)$  reaction were used as the standard to perform the  $(n,\alpha)$  reaction measurement. Present results are compared with existing measurements, evaluations and TALYS-1.6 code calculations.

## I. INTRODUCTION

Cross section data for the charged particle emitted reactions induced by the fast neutron are important both in basic nuclear physics and nuclear engineering applications. Samarium isotopes are relatively high-yield fission products in nuclear reactors. The  $(n,\alpha)$  reactions, in particular, are gas-producing and exothermic ones. The helium gas accumulated in the material will cause serious embrittlement problems [1].

Experimental measurements, however, are rather scanty for  $^{144}\text{Sm}(n,\alpha)^{141}\text{Nd}$  reaction. Only two measurements exist for neutron energies around 14 MeV, and there are large differences between them [2]. The two measurements were performed utilizing activation method [3-4]. Although most of evaluated nuclear data libraries contain this reaction, large discrepancies exist among them both in the trend and magnitude [5]. So, accurate measurements are demanded to address the application needs and clarify exciting discrepancies among different libraries.

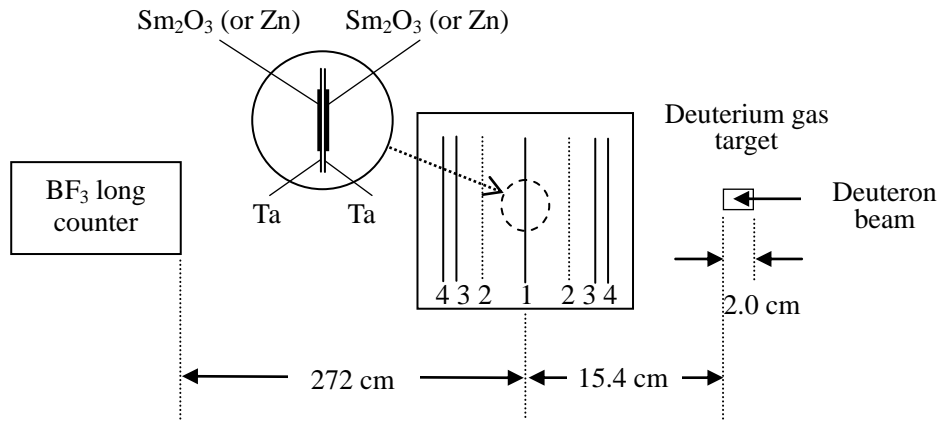
Natural Samarium is composed of seven isotopes, i.e.  $^{144}\text{Sm}(3.07\%)$ ,  $^{147}\text{Sm}(14.99\%)$ ,  $^{148}\text{Sm}(11.24\%)$ ,  $^{149}\text{Sm}(13.82\%)$ ,  $^{150}\text{Sm}(7.38\%)$ ,  $^{152}\text{Sm}(26.75\%)$  and  $^{154}\text{Sm}(22.75\%)$  [6]. We have measured the cross sections of the  $^{147}\text{Sm}(n,\alpha)^{144}\text{Nd}$  reaction at  $E_n = 5.0$  and  $6.0$  MeV, the  $^{149}\text{Sm}(n,\alpha)^{146}\text{Nd}$  reaction at  $E_n = 4.5, 5.0, 5.5, 6.0$  and  $6.5$  MeV [7-9].

## II. DETAILS OF EXPERIMENTS

The experiments were performed at the 4.5-MV Van de Graaff accelerator of Peking University, China. As shown in Fig. 1, the experimental apparatus consists of three main parts: the neutron source, the charged particle detector (with samples inside) and the neutron flux monitor.

A deuterium gas target was used to produce the monoenergetic neutron through the  ${}^2\text{H}(d,n){}^3\text{He}$  reaction. The deuterium gas cell is 2.0 cm in length and 0.9 cm in diameter which is separated from the beam-line vacuum by molybdenum foil 5.0  $\mu\text{m}$  in thickness. For neutrons with energy of 4.0, 5.0, and 6.0 MeV, the energy of the incident deuterium ions before entering the molybdenum foil was 1.78, 2.44, and 3.27 MeV, respectively. The corresponding neutron energy spreads ( $1\sigma$ ) were 0.23, 0.16, and 0.12 MeV, respectively [9]. During the experiment, the deuterium gas pressure was 3.0 atm and the incident deuteron beam current was about 3.0  $\mu\text{A}$ .

The  $\alpha$ -particle detector is a double-section gridded ionization chamber (GIC) with a common cathode, and its structure can be found in Ref. [14]. The distance from the cathode to the grid was 61 mm, and that from grid to anode 15 mm. Working gas of the GIC was Kr + 2.83%  $\text{CO}_2$ . The gas pressures during measurements are listed in Table I. High voltages applied on the cathode and anode are also included in Table I (the grids electrodes were grounded) which allowed complete collection of electrons from the ionization tracks.



1 Cathode; 2 Grid; 3 Anode; 4 Shield.

Fig. 1. Experimental setup.

Table I. Working, and of the GIC.

$E_n(\text{MeV})$	gas pressures (atm)	cathode high voltage (V)	anode high voltage (V)
4.0	1.55	-2400	1200
5.0	2.00	-2600	1300
6.0	2.00	-2600	1300

The  $^{144}\text{Sm}_2\text{O}_3$  samples were prepared by sedimentation method. The samples should be thin enough in order to reduce the energy loss and self-absorption of  $\alpha$ -particle in the sample material. In addition, big area samples are needed because the cross sections to be measured are small and the strengths of the neutron sources in the MeV region are limited. The number of  $^{144}\text{Sm}$  atoms in the samples was determined by weighing with an accuracy of 1  $\mu\text{g}$ . Data of the samples are listed in Table II.

A sample changer was set at the common cathode of the ionization chamber with five sample positions, and back-to-back double samples can be placed at each of them [14]. The  $^{144}\text{Sm}_2\text{O}_3$  samples were attached to the tantalum backings 0.1 mm in thickness. With back-to-back samples, forward ( $0^\circ\sim 90^\circ$ ) and backward ( $90^\circ\sim 180^\circ$ ) emitted  $\alpha$ -particles can be detected simultaneously.

Table II. Description of the samples.

Samples	Material	Isotopic abundance (%)	Thickness ( $\mu\text{g}/\text{cm}^2$ )	Diameter (mm)
$^{144}\text{Sm}$	$^{144}\text{Sm}_2\text{O}_3$	95.0	4300 <sup>a</sup> and 3370 <sup>b</sup>	44.0 <sup>a</sup> and 44.0 <sup>b</sup>
$^{238}\text{U}$	$^{238}\text{U}_3\text{O}_8$	99.999	493.6( $^{238}\text{U}$ only)	45.0

<sup>a</sup>Forward sample. <sup>b</sup> Backward sample.

A  $^{238}\text{U}$  film sample described in Table II was placed in the GIC at the forward direction to determine the absolute neutron flux by measuring the fission fragments. Double tantalum sheets and double compound alpha sources were also placed at other sample positions for (forward and backward) background measurements and energy calibrations, respectively.

The neutron flux monitor is a  $\text{BF}_3$  long counter. The axis of the counter was along the normal line of the electrodes of the ionization chamber as well as the  $0^\circ$  direction of the deuteron beam line. As shown in Fig. 1, the distance from the cathode of the chamber to the center of the deuterium gas cell was 15.4 cm, and that from the front side of the counter to the center of the gas cell was 272 cm.

Two-dimensional spectra of the cathode-anode coincidence signals for forward and backward directions were recorded separately, from which the number of  $\alpha$ -events from the measured ( $n,\alpha$ ) reactions can be obtained. The data-acquisition system (DAQS) can be found in Ref. [13]. At neutron energy point  $E_n = 4.0, 5.0$  and  $6.0$  MeV, the beam duration was 46, 31 and 26 h, respectively.

Since the  $^{238}\text{U}(n,f)$  reaction were used as the standard to perform the measurement, the cross section  $\sigma$  of the ( $n,\alpha$ ) reaction can be calculated by the following equation:

$$\sigma = \sigma_f \cdot \frac{N_\alpha / \epsilon_\alpha \cdot N_{^{238}\text{U}} \cdot N_{\text{BF}_3-f}}{N_f / \epsilon_f \cdot N_{^{144}\text{Sm}} \cdot N_{\text{BF}_3-\alpha}}. \quad (1)$$

The  $\sigma_f$  is the standard  $^{238}\text{U}(n,f)$  cross sections taken from ENDF/B-VII.1 library [5]. The  $N_\alpha$  and  $N_f$  are the detected counts above the energy threshold from the  $(n,\alpha)$  reaction (after background subtraction) and from the  $^{238}\text{U}(n,f)$  reaction, respectively. The  $\varepsilon_\alpha$  and  $\varepsilon_f$  are the detection efficiency for  $\alpha$ -particles and fission fragments. The  $N_{238\text{U}}$  and  $N_{144\text{Sm}}$  are the numbers of  $^{238}\text{U}$  and  $^{144}\text{Sm}$  nuclei in the samples, respectively,  $N_{\text{BF}_3-f}$  and  $N_{\text{BF}_3-\alpha}$  are the counts of the neutron flux monitor ( $\text{BF}_3$  counter) for  $^{238}\text{U}$  fission and for  $(n,\alpha)$  event measurements, respectively.

The detection efficiency for  $\alpha$ -particles  $\varepsilon_\alpha$  and fission fragments  $\varepsilon_f$  can be written as

$$\varepsilon = \frac{N_{det}}{N_{det} + N_{th} + N_{ab}}, \quad (2)$$

Where  $N_{det}$  is the detected counts, i.e.  $N_\alpha$  or  $N_f$ ,  $N_{th}$  is the number of events with amplitudes below threshold (the threshold correction), and  $N_{ab}$  is the number of events absorbed in the samples (the self-absorption correction) [16]. The calculation method of  $\varepsilon$  will be discussed in the next section.

The cross sections of the  $^{144}\text{Sm}(n,\alpha)^{141}\text{Nd}$  reaction in forward and backward directions can be calculated separately using equations (1) and (2). The complete cross section can be obtained by adding them up together.

### III. DATA PROCESSING, RESULTS, AND DISCUSSIONS

The data processing methods are almost the same for both  $(n,\alpha)$  reactions to be measured at all neutron energies. As an example, the following descriptions are given for the data processing of the  $^{144}\text{Sm}(n,\alpha)^{141}\text{Nd}$  at  $E_n = 4.0$  MeV reaction for the forward direction.

Firstly, two-dimensional spectrum of compound  $\alpha$ -sources was obtained used for energy calibration and valid-event-area determination. The four groups of  $\alpha$  particles, i.e.  $\alpha_1$ ,  $\alpha_2$ ,  $\alpha_3$ ,  $\alpha_4$  as shown in Fig. 2, are emitted from  $^{234}\text{U}$ ,  $^{239}\text{Pu}$ ,  $^{238}\text{Pu}$  and  $^{244}\text{Cm}$  alpha sources with energies of 4.775, 5.155, 5.499, 5.805 MeV, respectively. The determined valid-event-area is between the  $0^\circ$  and  $90^\circ$  curves as shown in Fig. 2.

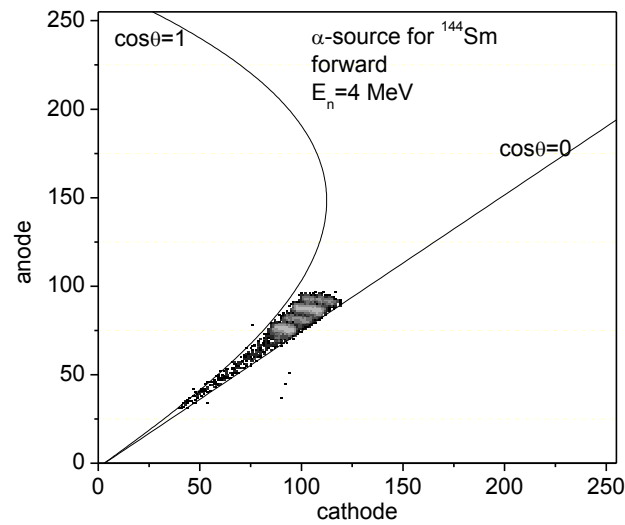


Fig. 2. Two-dimensional spectrum of the compound  $\alpha$  sources.

Secondly, cathode-anode two-dimensional spectra for the foreground and background are obtained from the experimental data. Due to the large Q value background measurement for the  $^{144}\text{Sm}(n,\alpha)^{141}\text{Nd}$  reaction were not made as shown in Figs. 3. The valid-event-area was used to pick out the expected  $\alpha$ -events from the  $^{144}\text{Sm}(n,\alpha)^{141}\text{Nd}$ . Figs. 5 shows the anode spectrum after the projection of the selected  $\alpha$ -events. As can be seen  $\alpha$ -events corresponding to different energy levels of the residual nuclei cannot be separated and they become one broad peak due to the close energy levels of the residual nuclei and the energy loss of  $\alpha$ -particles in the sample. The  $\alpha$  counts above the threshold can be obtained from the anode spectrum.

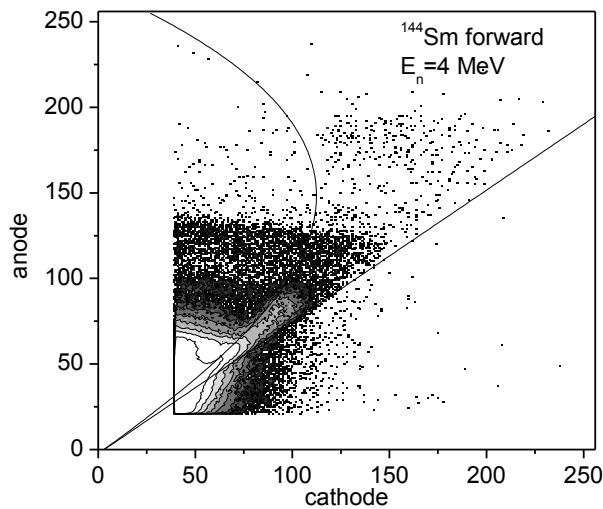


Fig. 3. Two-dimensional spectrum of the  $^{144}\text{Sm}(n,\alpha)^{141}\text{Nd}$  reaction at  $E_n = 4.0 \text{ MeV}$  (forward).

As shown in Fig. 4 and, in addition to the  $\alpha$  counts above threshold, there are also  $\alpha$  events below the threshold which cannot be detected. Therefore, threshold and self-absorption corrections are needed. To determine the detection efficiency of  $\alpha$ -particle, the anode spectra were simulated as shown in Figs. 4 with the dashed curves. The SRIM code was used to get the stopping power of  $\alpha$ -particles in the samples, and the TALYS-1.6 code to predict the angular and energy distributions of the emitted  $\alpha$ -particles [17-18]. To obtain the well fitted anode spectrum, level densities from Hilaire's combinatorial tables (Id model 5 in TALYS) were used when use the TALYS-1.6 code to predict the angular and energy distributions of the emitted  $\alpha$ -particles for the  $^{144}\text{Sm}(n,\alpha)^{141}\text{Nd}$  reaction.

The corrected  $\alpha$  counts is obtained through the division of  $\alpha$  counts above threshold and the correction factor, which is calculated through the simulated anode spectra. The calculated correction factor value is from 77% to 82%.

The fission counts can be obtained from the anode spectrum of the fission fragments from the  $^{238}\text{U}(n, f)$  reaction. The anode spectrum at  $E_n = 6.0 \text{ MeV}$  is shown in Fig. 5. To determine the detection efficiency of fission fragments, threshold and self-absorption corrections were made by Monte Carlo simulation using the fission product yield data from the ENDF/B-VII.1 library[5]. The dashed curve in Fig. 5 shows the simulated result for the fission fragments with low energy.

The detection efficiency for fission fragments is from 85% to 92%. Using the standard  $^{238}\text{U}(n,f)$  cross sections, the neutron flux can be determined with an uncertainty of 5.0.

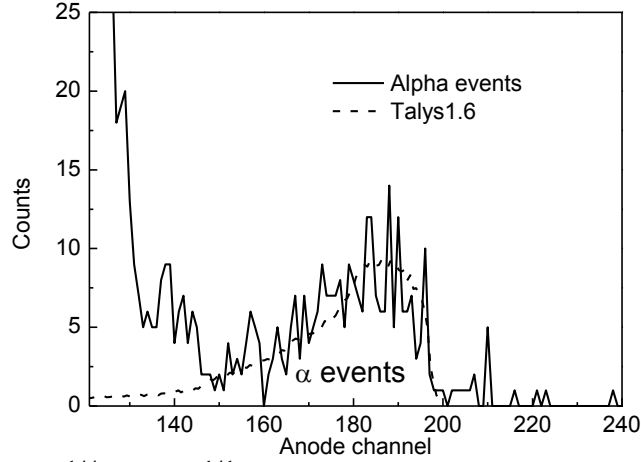


Fig. 4. Anode spectrum of the  $^{144}\text{Sm}(n,\alpha)^{141}\text{Nd}$  reaction at  $E_n = 4.0$  MeV (forward direction).

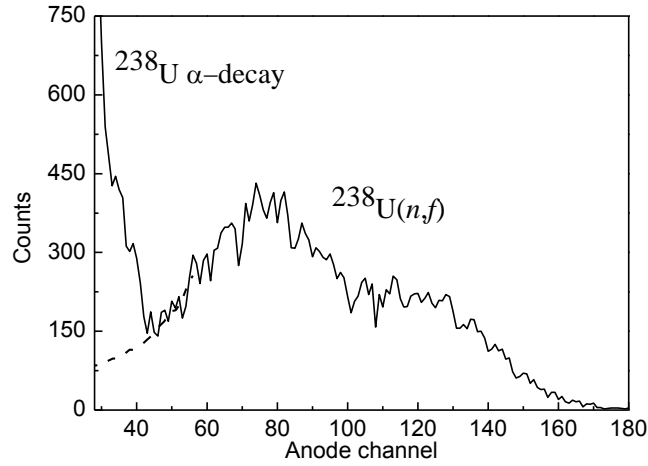


Fig. 5. Anode spectrum of the  $^{238}\text{U}$  fission fragments at  $E_n = 6.0$  MeV.

The measured results of the cross section for the  $^{144}\text{Sm}(n,\alpha)^{141}\text{Nd}$  reaction are listed in Table III. The calculated results using the TALYS-1.6 code with default and adjusted parameters are also listed in Table III. Parameters of the optical model potential were adjusted to obtain a good agreement with present results. For the  $^{144}\text{Sm}(n,\alpha)^{141}\text{Nd}$  reaction, the factor of geometry radius parameter,  $r_v$ , were adjusted from 1 (the default) to 0.8 and the constant  $c$  of the adjustment function for tabulated level densities were adjusted from 1 (the default) to 0.3. The adjustable range of the parameter  $r_v$  and  $c$  is from 0.1 to 10 and from -10 to 10, respectively [18].

The uncertainty was calculated using the error propagation formula. Sources of uncertainty and their magnitudes are listed in Table IV. Major source of uncertainty is the counting error for  $\alpha$  particles (including statistics and background subtraction) produced by the valid-event-area cut and the energy threshold cut. The uncertainty of detection efficiency for  $\alpha$  particles is due to the threshold and self-absorption correction based on Talys-1.6 code. Numbers of  $^{144}\text{Sm}$  and  $^{238}\text{U}$  nuclei were determined by the mass weighing with the precision up to  $1\mu\text{g}$  and the uncertainty of the numbers of nuclei is less than one percent.

Table III. Measured and Talys-1.6 calculated cross sections for the  $^{144}\text{Sm}(n,\alpha)^{141}\text{Nd}$  reaction.

$E_n$ (MeV)	$\sigma_{\text{exp}}$ (mb)	$\sigma_{\text{Talys}}$ (mb)
4.0	$0.06 \pm 0.01$	$0.11^{\text{i}}, 0.08^{\text{ii}}$
5.0	$0.11 \pm 0.03$	$0.15^{\text{i}}, 0.11^{\text{ii}}$
6.0	$0.17 \pm 0.03$	$0.22^{\text{i}}, 0.17^{\text{ii}}$

<sup>i</sup> Predictions of TALYS-1.6 with default parameters.

<sup>ii</sup> Predictions of TALYS-1.6 with adjusted parameters.

Table IV. Sources of uncertainty and their magnitudes.

Sources of uncertainty	Magnitude (%)
Counting uncertainty for $\alpha$ particles	20-30
Detection efficiency for $\alpha$ particles	10.0
Fission counts of $^{238}\text{U}$	4.0
Normalization of the $\text{BF}_3$ counts	1.5
Numbers of $^{144}\text{Sm}$ nucleus	1.0
Numbers of $^{238}\text{U}$ nucleus	1.3
$^{238}\text{U}(n,f)$ cross sections	1.0

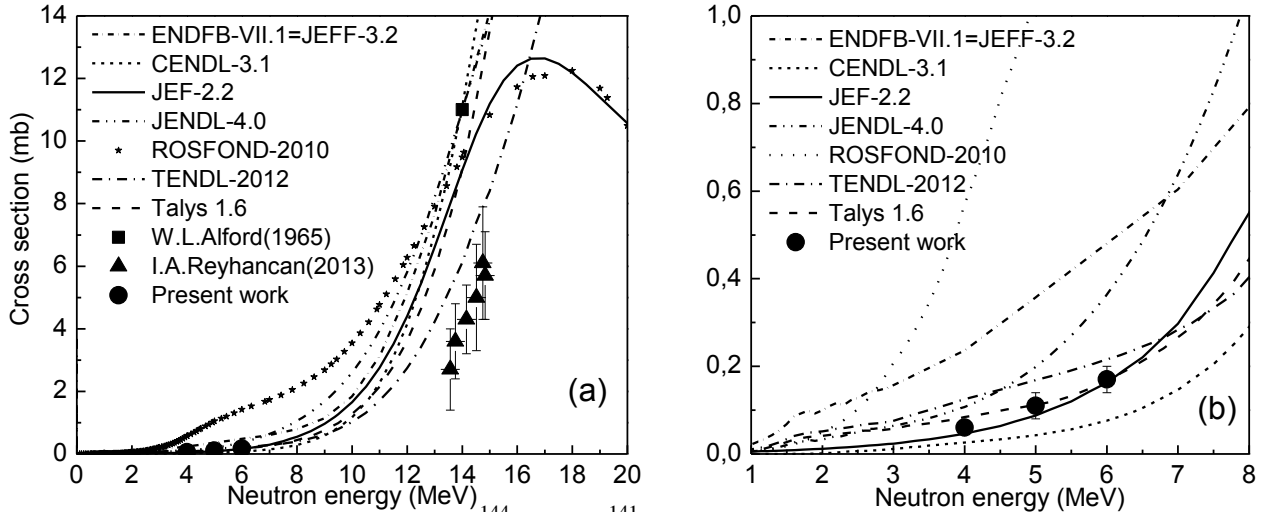


Fig. 6. Present cross sections of the  $^{144}\text{Sm}(n,\alpha)^{141}\text{Nd}$  reaction compared with existing measurements and evaluations for neutron energy region (a) from 0 to 20 MeV and (b) from 1.0 to 8.0 MeV.

Results of the present work are compared with those of existing measurements, evaluations, and TALYS-1.6 calculations as shown in Figs. 6, only two measurements exist with big uncertainties for neutron energies around 14 MeV. Except for TENDL-2012, most other evaluation libraries go toward the Alford's data point [3]. There are large deviations among different evaluation libraries in the MeV region. Our measurements support the data of JEF-2.2 libraries. The TALYS-1.6 calculations agree well with our measurements as well as the Alford's result. Further measurements at neutron energies about 10 MeV are necessary to clarify the discrepancies among different libraries.

#### IV. CONCLUSIONS

In the present work, the cross section for the  $^{144}\text{Sm}(n,\alpha)^{141}\text{Nd}$  reaction were measured at  $E_n=4.0, 5.0$  and  $6.0$  MeV. Our results are generally in agreement with TALYS-1.6 calculations. Our measurements support the data of JEF-2.2 libraries. Further measurements are needed at

neutron energies from 8 to 12 MeV to clarify the discrepancies among different libraries.

#### ACKNOWLEDGEMENTS

The authors are indebted to the operation crew of the 4.5-MV Van de Graaff accelerator of Peking University. The present work was financially supported by the National Natural Science Foundation of China (11175005 and 11475007).

#### REFERENCES

1. M.B. Chadwick, E. Dupont, E. Bauge, A. Blokhin, et al., Nuclear Data Sheets, **118**, 1 (2014).
2. EXFOR: Experimental Nuclear Reaction Data, database version of September 02, 2015, <https://www-nds.iaea.org/exfor/exfor.htm>
3. W.L. Alford, R.D. Koehler, Bulletin of the American Physical Society, **10**, 260 (1965).
4. I.A. Reyhancan, A. Durusoy, Nuclear Science and Engineering, **174**, 202 (2013).
5. ENDF: Evaluated Nuclear Data File, database version of September 02, 2014, <https://www-nds.iaea.org/exfor/endl.htm>
6. NuDat2, National Nuclear Data Center, Brookhaven National Laboratory, version 2.6, <http://www.nndc.bnl.gov/nudat2>
7. Yu.M. Gledenov, M.V. Sedysheva, V.A. Stolupin, Guohui Zhang, Jiaguo Zhang, Hao Wu, Jiaming Liu, Jinxiang Chen, G. Khuukhenkhuu, P. E. Koehler, P. J. Szalanski, Phys. Rev. C, **80**, 044602 (2009).
8. Yu.M. Gledenov, Guohui Zhang, G. Khuukhenkhuu, M.V. Sedysheva, P.J. Szalanski, P.E. Koehler, Jiaming Liu, Hao Wu, Xiang Liu, Jinxiang Chen, Phys. Rev. C, **82**, 014601 (2010).
9. Guohui Zhang, Yu.M. Gledenov, G. Khuukhenkhuu, M.V. Sedysheva, P.J. Szalanski, P.E. Koehler, Y.N. Voronov, J. Liu, X. Liu, J. Han, J. Chen, Phys. Rev. Lett., **107**, 252502 (2011).
10. Guohui Zhang, Rongtai Cao, Jinxiang Chen, Guoyou Tang, Yu.M. Gledenov, M. Sedysheva, G. Khuukhenkhuu, Nucl. Science and Eng., **156**, 115 (2007).
11. Guohui Zhang, Jiaguo Zhang, Rongtai Cao, Li'an Guo, Jinxiang Chen, Yu.M. Gledenov, M.V. Sedysheva, G. Khuukhenkhuu, P.J. Szalanski, Nucl. Science and Eng., **160**, 123 (2008).
12. Guohui Zhang, Yu.M. Gledenov, G. Khuukhenkhuu, M.V. Sedysheva, P.J. Szalanski, Jiaming Liu, Hao Wu, Xiang Liu, Jinxiang Chen, V.A. Stolupin, Phys. Rev. C, **82**, 054619 (2010).
13. Guohui Zhang, Hao Wu, Jiaguo Zhang, Jiaming Liu, Yu.M. Gledenov, M.V. Sedysheva, G. Khuukhenkhuu, P.J. Szalanski, Eur. Phys. J. A, **43**, 1 (2010).
14. X. Zhang, Z. Chen, Y. Chen, J. Yuan, G. Tang, G. Zhang, J. Chen, Y.M. Gledenov, G. Khuukhenkhuu, M. Sedysheva, Phys. Rev. C **61**, 054607 (2000).
15. Q-value calculator, National Nuclear Data Center, Brookhaven National Laboratory, <http://www.nndc.bnl.gov/qcalc/>
16. Yu.M. Gledenov, M.V. Sedysheva, V.A. Stolupin, Guohui Zhang, Jinhua Han, Zhimin Wang, Xiao Fan, Xiang Liu, Jinxiang Chen, G. Khuukhenkhuu, P.J. Szalanski, Phys. Rev. C, **89**, 064607 (2014).
17. J.F. Ziegler, SRIM-2013, <http://www.srim.org/#SRIM>.
18. A.J. Koning, S. Hilaire, and M.C. Duijvestijn, "TALYS-1.0", *Proceedings of the International Conference on Nuclear Data for Science and Technology*, April 22-27, 2007, Nice, France, editors O. Bersillon, F. Gunsing, E. Bauge, R. Jacqmin, and S. Leray, EDPSciences, 2008, p. 211-214.